Available online at www.sciencedirect.com
SCIENCE DIRECT®
Chemical Physics Letters 396 (2004) 393–397
CHEMICAL PHYSICS LETTERS
www.elsevier.com/locate/cplett

Sub-wavelength localization of hot-spots in SERS

E.C. Le Ru, P.G. Etchegoin *

School of Chemical and Physical Sciences, The McDiarmid Institute for Advanced Materials and Nanotechnology, Victoria University of Wellington, P.O. Box 600, Wellington, New Zealand

Received 28 July 2004; in final form 17 August 2004

Abstract

Localization of plasmon resonances within fractions of the wavelength of the exciting laser is shown by means of surface enhanced Raman scattering (SERS). Our results confirm speculations on sub-wavelength resolution capabilities of SERS as well as provide a tool to understand highly localized plasmon excitations in disordered metallic nanostructures. It also provides some insight into the nature of hot-spots, believed to be responsible for the huge amplifications seen in single molecule SERS.

Surface enhanced Raman scattering (SERS) [1] is based on single or collective plasmon resonances producing massive amplifications of the laser local field, thus boosting the intensity of the otherwise weak Raman scattering scattering process. This is the so-called electromagnetic (EM) enhancement. A second source of enhancement (chemical) [2] is always present, but plays a secondary role when huge amplifications are observed. Understanding SERS, accordingly, implies an understanding of the nature of collective plasmon resonances in the metallic nanostructures where the effect is observed. This is a very difficult undertaking in general.

The largest SERS signals are believed to come from the so-called *hot-spots*; spatially localized surface plasmons resonances where the electric field of the laser may reach huge local enhancements. Hot-spots are in many cases directly related to two-particle interactions (dimers) in colloidal systems, but there are many theoretical reasons to believe that they can also be produced by collective excitations, with a much more indirect relationship with the underlying topology of the metal nanostructure. It is believed that hot-spots are responsible for the single-molecule (SM) sensitivity of SERS [3]; understanding their physical properties is at the core of the possible applications of SERS in SM-spectroscopy. It has been argued repeatedly in the literature that hot-spots could be spatially localized within a fraction of the laser wavelength (λ) [3]. This is a property which is interesting for several reasons: (i) it says something about the nature of plasmon resonance localization which is important for plasmonics itself [4–6]; (ii) it could explain the existence of huge ($\sim 10^{12}$–10^{15}) EM enhancements which are needed to explain many SM or alleged SM-phenomena and (iii) it could set the limits of spatial (sub-wavelength) resolution in SERS as an alternative tool for microscopy with high chemical specificity.

Although some information on the spatial localization of hot-spots has been obtained in the past with alternative techniques [7,8], a clear-cut experimental demonstration of sub-wavelength localization of hot-spots inferred from the direct monitoring of the Raman signal has not been yet demonstrated in the literature, to the very best of our knowledge. It is the purpose of this Letter to present such evidence; i.e., sub-wavelength confinement of hot-spots and spatial resolution within distances smaller than λ. We demonstrate, accordingly,

* Corresponding author.
E-mail addresses: Eric.LeRu@vuw.ac.nz (E.C. Le Ru), Pablo.Etchegoin@vuw.ac.nz (P.G. Etchegoin).

0009-2614/$ - see front matter © 2004 Elsevier B.V. All rights reserved.
doi:10.1016/j.cplett.2004.08.065

a new tool that can be used to further our understanding of the causes of plasmon-mediated EM-enhancement in a technique that is becoming of age in many applications in physics [9], chemistry [10], physical-chemistry [11], and biology [3,12].

A modern Raman spectrometer with a single dispersing stage works by achieving a high rejection of laser stray light in a holographic notch filter. Detection is typically achieved by a CCD array, which is essentially a two-dimensional detector where there is both: (i) frequency and (ii) spatial information of the imaged object (laser spot) at the entrance slit. When coupled to a confocal microscope, the system achieves an image of the laser spot onto the entrance slit of the spectrometer. The situation is depicted schematically in Fig. 1a. The grating disperses the image onto the CCD; the intensity pattern can be thought of as containing frequency (energy) information in the direction perpendicular to both the slits and the grooves of the grating, and spatial information in the parallel direction. Only one direction of the image object is spatially resolved, while the others (including the axial direction) are spread into the different frequency components contained in the image. This is schematically shown as *frequency* and *position* axes in Fig. 1a. The normal mode of operation of a spectrometer is by integrating the position-axis in columns for every frequency. This can be setup and/or changed by the so called *binning* of the diodes in the CCD.

The spatial resolution dependence of the CCD Raman image can be tested for *any* specific system by scanning the tightly focused laser spot of the confocal microscope through a cleaved silicon wafer edge on top of a neutral highly-absorbing substrate. An example is shown in Fig. 1b. From Fig. 1a it is obvious that the CCD image is only sensitive to spatial inhomogeneities in one direction.

The grooves (lines) of the grating define a specific direction. The Si wafer edge can be moved so that the image of the edge itself remains all the time either parallel or perpendicular to the direction defined by the grooves. The relation between the directions on the sample and the directions in the image depends on the optical layout creating the image on the entrance slit. If the edge remains parallel to the grooves at all times, there is no spatial information on the Raman image. This is explicitly shown in Fig. 1c where the Raman peak of Si ($\sim$520 cm^{-1}) always appears in the same vertical position, though with different intensities, for a 633 nm He–Ne-laser spot crossing the cleaved edge. The beam has a full width at half maximum (FWHM) at the waist of 650 nm measured independently by beam profiling techniques. The intensity pattern in the vertical (spatial) direction in Fig. 1a simply follows a Gaussian distribution, which is the illumination pattern of the beam. If the edge is scanned in the direction perpendicular to the grooves of the grating, the CCD-Raman image

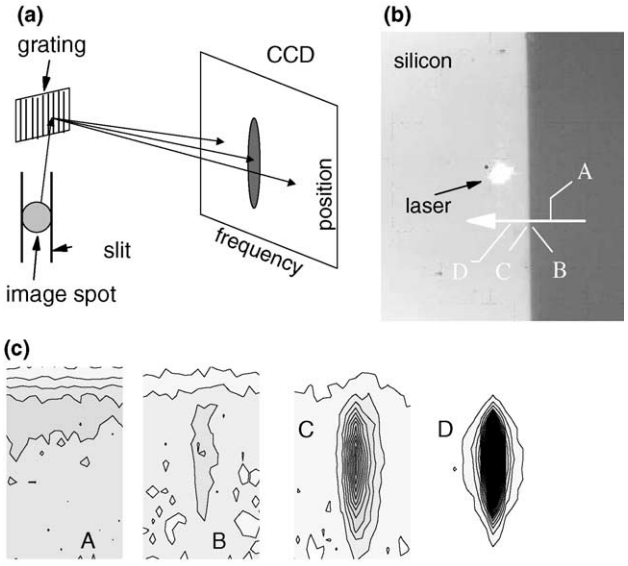

Fig. 1. (a) Schematic representation of a single-path Raman spectrometer after the notch filter and the confocal pinhole (not shown in the figure). A confocal image of the spot is formed onto the entrance slit by the collecting optics. The grating disperses (spectrally) the image onto the CCD achieving a combined intensity pattern with both spatial (position) and frequency information in the two mutually perpendicular directions of the CCD. (b) A laser spot (FWHM $\sim\lambda$) is scanned across a Si cleaved edge as shown in the picture. Depending on the orientation of the edge ($\parallel$ or $\perp$ to the grooves of the grating) a Raman CCD image can be obtained with ($\perp$) or without ($\parallel$) spatial variations. (c) A scanning across the *insensitive* spatial direction of the CCD ($\parallel$ to the grooves) produces always a centered Raman image pattern with a Gaussian profile. The maximum intensity of the pattern is a measure of the fraction of the area of the spot on the Si wafer, but no spatial variation is detected in this case. From left to right the images are for: zero (A), 1/4 (B), 1/2 (C) and full (D) overlap of the spot on the wafer. As in (a), the horizontal axis is frequency while the vertical direction is the spatial coordinate.

shows now a spatial variation. This is displayed in Fig. 2 where the spot is scanned through two cleaved edges of the Si wafer. If the beam is now missing a fraction of its left or right side across the edge, this results in a Raman image on the CCD which is slightly displaced upwards or downwards. In this manner, under careful focusing conditions, events occurring within the laser spot can be spatially separated and resolved for distances of the order of $\sim\lambda/2$, which is the diffraction limit. Figs. 1 and 2, therefore, underline all the basic physical and instrumental concepts which can be transferred to an arbitrary Raman system with a confocal microscope, a CCD detector, and a motorized X–Y sample stage. The stability of the laser beam (spatial and intensity) can also be tested by monitoring the CCD-Raman images on Si. We find good long term spatial (Gaussian) and temporal (intensity) stability in our laser.

The CCD-Raman image of a peak has two different widths: (i) in the frequency direction it is the linewidth of the Raman peak itself and the relation between wavenumbers and pixels is fixed by the dispersion of the grat-

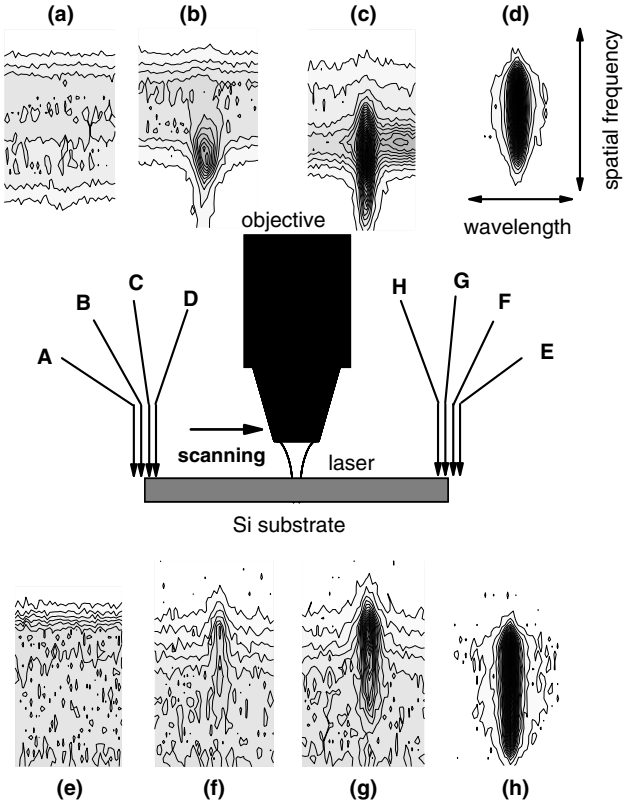

Fig. 2. Scanning the laser spot across a cleaved edge in the direction parallel to the grating grooves produces a Raman image pattern where spatial resolution can be observed. A Si wafer (50 μm thick) on top of an absorbing substrate is cleaved with two edges separated by a few mm only and scanned across the spot produced by the objective (center). The CCD Raman images of the Si signal are shown at the top and bottom of the figure, with the corresponding letter that identifies the specific place where the signal has been taken from. The scanning direction is indicated in the figure. A spot missing a fraction of its left (right) area produces a CCD-Raman image slightly displaced downwards (upwards). In this manner, we can distinguish signals within the spot separated by a distance of the order of $\sim\lambda/2$, which is the diffraction limit.

ing. In the *spatial* or *position* axis, the shape of the image is a Gaussian which comes from the Gaussian shape of the beam. If the beam size (FWHM) is known at the spot site, a Gaussian fit of the intensity on the CCD image automatically sets a connection between pixels and distance.

Not many samples will have Raman signals with strong inhomogeneities within distances $\sim\lambda$. SERS provides a prototype example due to the presence of hot-spots. We take a classical example in SERS to prove the method: residual amorphous carbon on silver colloids.

Experiments have been performed on a Jobin–Yvon LabRam system coupled to an Olympus BX41 confocal microscope equipped with achromatic 100× objectives either for immersion (water) or air. We fixed the confocal pinhole to 200 μm for all measurements providing a confocal length of ~8 μm in the axial direction. Raman spectra are collected either in the normal spectroscopic mode or as CCD Raman images with a 633 nm He–Ne-laser (~3 mW at the focal point). Ag colloids for SERS were prepared by reduction of $AgNO_3$ using the standard technique introduced by Lee and Miesel [13] and concentrated 10 times by centrifugation (10 min at 15×10^3 rpm) from the neat solution ($\sim10^{11}$ colloids/cm^3). The average colloid diameter is ~60 nm as revealed by dynamic light scattering in solution and electron microscopy on dry samples. The concentrated colloids are dried onto glass slides for several hours under mild heating (~40 °C).

It is a well known fact that pure colloids prepared by this method have a substantial amount of residual amorphous carbon which can be easily identified in the SERS spectrum [14]. Kudelski and Pettinger [15] have done a detailed study of SERS in amorphous carbon and carbon chain segments. They have shown [15] that on top of the broad double peak at ~1360 and ~1580 cm^{-1}, characteristic of many forms of amorphous carbon, it is possible to have fluctuations in the Raman peaks corresponding to carbonaceous groups which get temporarily amplified by hot-spots in an enduring surface chemistry process triggered by the laser [15]. These photochemical reactions are interesting in their own right, and are seen at relatively low laser powers (~2 mW); they change dynamics and become more complicated at higher powers. A full separate study of the photochemistry of amorphous carbon under SERS conditions is in progress and will be reported elsewhere. The fluctuations of these groups can be readily seen in our sample, as demonstrated in Fig. 3a. The Raman spectrum of average amorphous carbon is shown for reference. It is the signal of all these carbon clusters that normally contributes to the inhomogeneous broadening of the peaks in amorphous carbon. SERS is resolving part of the inhomogeneous broadening by amplifying specific clusters only; those at the hot-spots.

If we analyze the CCD-Raman image in the same spectral range, we observe that each spectrum at each given time (obtained with the normal binning in the spatial direction of the CCD) shown in Fig. 3a is actually composed of several spectra which are substantially different among regions within the spot, as shown in Fig. 3b. This does not obviously occur at every position, but it is possible to find many places where the Raman signal is inhomogeneous within the spot. This is specifically shown in the example in Fig. 3b where the FWHM of the beam on the sample is, as before, 650 nm $\sim\lambda$. This proves that different regions within the spot have not only different enhancements but also different spectra; we are resolving inhomogeneities in the SERS signal for distances smaller than λ.

Fractal-like clusters of dried Ag-colloids on glass can, however, be relatively uniform in terms of average enhancement over regions which are large compared

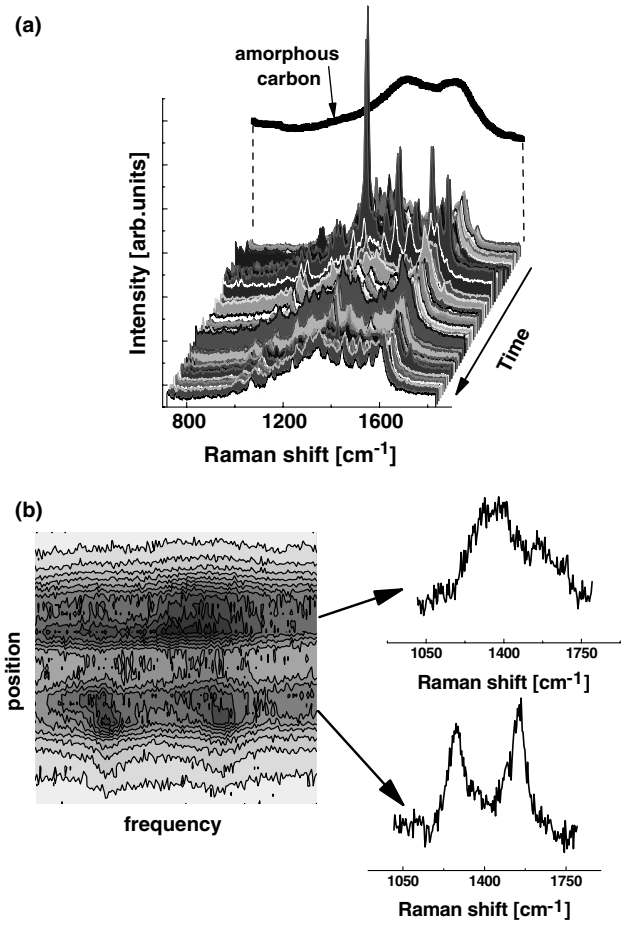

Fig. 3. (a) Amorphous carbon (a-C) fluctuations seen on Ag-colloid clusters. The time scan corresponds to 250 spectra taken with 1 s integration time each. The average spectrum of a-C is shown at the back for reference. On top of a background resembling the average spectrum of a-C, there are huge fluctuations in the SERS signal produced by carbonaceous groups [15] at hot-spots. (b) CCD-Raman image centered in the same spectral range, but spatially resolved within the spot. The vertical position spans a range of approx 650 nm obtained from a fit of the Si-profile. The image shows regions with very different Raman spectra along the spatially resolved direction, as shown in the two examples on the right. See the text for further details.

to the spot size. More spectacular spatial inhomogeneities of hot-spots can be seen in small clusters of Ag-colloids in solution (water) containing rhodamine 6G (RH6G). The small clusters are produced by a partial collapse of the Ag-colloid stability triggered by the presence of KCl [16,17] (10–20 mM). Transient SERS signals of clusters getting into the scattering volume are measured in the same experimental conditions as reported elsewhere [16,17] but with a higher magnification (×100) immersion objective index-matched to water. CCD-Raman images in the region close to one of the most intense modes of RH6G (~1510 cm^{-1}) show all possible cases of different localizations of strong Raman signals within the laser spot. Fig. 4 shows three examples of events where there was an off-center hot-spot during the time of the measurement (0.1 s) (left), a centered intense one (center) and an event with two hot-spots one slightly weaker than the other (right). Again this example shows that conventional binning in these cases of strong hot-spot inhomogeneities will produce an average signal of regions where the Raman spectra looks quite different. The images in Fig. 4 also give some hint on the time-scale of hot-spot resonance occurrences in these clusters. With an integration time of 0.1 s and a readout time of the order of ~1 s, many hot-spots appear very localized in the image (as the three examples in Fig. 4c). This suggests that they are transient resonances of the clusters occurring on a much smaller time scale when a specific position or relative orientation of the cluster with respect to the laser beam is achieved. The only reason why this experiment cannot provide a definite answer to this question is the wrapping of two of the spatial dimensions, which could be hiding a diffusion process and blurring along the insensitive spatial directions.

Spatial localization of hot-spots studied by this method has the advantage of spectroscopic information combined with some degree of spatial resolution in one direction. However, at the focal plane, one of the dimensions is wrapped along the spatially insensitive axis (frequency axis) of the CCD. There is however an alternative which could provide a two dimensional sub-wavelength SERS information by resigning some resolution and specificity in the spectral dimension. The Raman imaging method proposed in [18], is based on a triple spectrometer using a double subtractive stage with an intermediate slit to filter the image on the entrance slit in a small energy window around a Raman mode of interest. The third stage is then used with a grating at 0 nm in reflection mode to provide a 2D-map, with spatial information on both axes from the image at the entrance slit, filtered by the double subtractive stage.

Sub-wavelength spatial resolution in SERS spectra has been demonstrated for two different experimental situations. Our results confirm speculations on the spatial localization of hot-spots in SERS. Unlike other techniques like photon scanning tunnelling microscopy [7], direct spatially resolved Raman imaging produces spectra in which both spatial and spectroscopic information within the laser spot can be obtained. We believe this imaging method to be sufficiently general to be applied to any other metallic nanostructures.

We have found, in addition, evidence that very localized photochemical reactions can be triggered by the presence of these hot-spots in colloidal clusters. The existence of surface plasmon enhanced mediated photochemistry is known already [19], but the possibility of localizing or even controlling these reactions by hot-spots open several interesting possibilities. We have found evidence of certain photochemical reactions

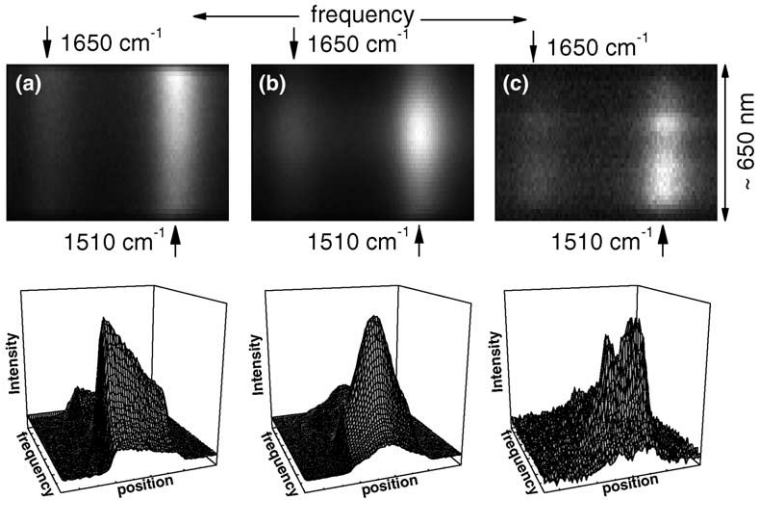

Fig. 4. CCD-Raman images of the spot with the immersion objective. The solution contains Ag-colloid clusters formed by the presence of 20 mM KCl and 1μM RH6G. All possible types of Raman hot-spots can be seen within the laser spot as a function of time. The integration time was 0.1 s for these images. Two clear features at ~1650 and 1510 cm^{-1} can be seen in all images. We show three representative examples with: (a) an off-axis hot-spot, (b) an intense hot-spot in the center of the beam, and (c) an event with two clearly resolved hot-spots separated by $\sim\lambda/2$. The three figures at the bottom present the same data in a 3D-plot, where the different asymmetries of the Raman signals in the spatial direction can be readily seen.

which show intense emission of light form sub-wavelength localized regions. Work along these lines is in progress and results will be reported elsewhere.

Acknowledgements

P.G.E. acknowledges support by the Engineering and Physical Sciences Research Council (EPSRC) of the UK under a travelling Grant (GR/T06124). We are indebted to Robert C. Maher (Imperial College London) for providing the colloids, and to Richard Tilley and David Flynn (Victoria University) for help with electron microscopy.

References

[1] M. Moskovits, Rev. Mod. Phys. 57 (1985) 783.
[2] A. Otto, in: M. Cardona, G. Güntherodt (Eds.), Light Scattering in Solids, Springer, Berlin, 1984, p. 289.
[3] K. Kneipp, H. Kneipp, I. Itzkan, R.R. Dasari, M. Feld, J. Phys. Condens. Matter 14 (2002) R597.
[4] M.I. Stockman, S.V. Faleev, D.J. Bergman, Phys. Rev. Lett. 87 (2001) 167401.
[5] D.J. Bergman, M.I. Stockman, Phys. Rev. Lett. 90 (2003) 027402.
[6] S. Zou, N. Janel, G.C. Schatz, J. Chem. Phys. 120 (2004) 10871.
[7] D.P. Tsai, J. Kovacs, Z. Wang, M. Moskovits, V.M. Shalaev, J.S. Suh, R. Botet, Phys. Rev. Lett. 72 (1994) 4149.
[8] P. Zhang, T.L. Haslett, C. Douketis, M. Moskovits, Phys. Rev. B 57 (1998) 15513.
[9] P. Etchegoin, L.F. Cohen, H. Hartigan, R.J.C. Brown, M.J.T. Milton, J.C. Gallop, J. Chem. Phys. 119 (2003) 5281.
[10] A.M. Michaels, M. Nirmal, L.E. Brus, J. Am. Chem. Soc. 121 (1999) 9932.
[11] R.C. Maher, L.F. Cohen, P. Etchegoin, Chem. Phys. Lett. 352 (2002) 378.
[12] H. Xu, E.J. Bjerneld, M. Käll, L. Börjesson, Phys. Rev. Lett. 83 (1999) 4357.
[13] P.C. Lee, D. Meisel, J. Phys. Chem. 86 (1982) 3391.
[14] A. Otto, J. Raman Spectros. 33 (2002) 593.
[15] A. Kudelski, B. Pettinger, Chem. Phys. Lett. 321 (2000) 356.
[16] P. Etchegoin, R.C. Maher, L.F. Cohen, H. Hartigan, R.J.C. Brown, M.J.T. Milton, J.C. Gallop, Chem. Phys. Lett. 375 (2003) 84.
[17] R.C. Maher, L.F. Cohen, P. Etchegoin, H.J.N. Hartigan, R.J.C. Brown, M.J.T. Milton, J. Chem. Phys. 120 (2004) 11746.
[18] P. Etchegoin, Phys. Rev. E 59 (1999) 1860.
[19] R.T. Kidd, D. Lennon, S.R. Meech, J. Chem. Phys. 113 (2000) 8276.